Effect of norbornene content on deformation properties and hot embossing of cyclic olefin copolymers

Patrick W. Leech · Xiaoqing Zhang ·
Yonggang Zhu

Abstract The dynamic mechanical behaviour of a series of cyclic olefin copolymers (COCs) with varying norbornene content has been examined in the vicinity of the glass transition temperature, T_g. Using dynamic mechanical thermal analysis (DMTA), the temperature of the glass transition in COC increased linearly with increase in % norbornene. Above T_g, the magnitude of the elastic storage modulus, E', decreased exponentially with rise in temperature for all of the copolymers. The loss modulus, E'', has also sharply decreased at temperatures above the transition with a levelling-off in E'' at ≥ 20 °C above T_g for all grades. The results of DMTA have been used in the identification of the optimum conditions for hot embossing experiments. Hot embossing of COC at ≥ 20 °C above the transition temperature in a region of viscous liquid flow has resulted in a full replication of channel depth without cracking or distortion.

Introduction

There has been growing interest in the use of cyclic olefin copolymer (COC) in microfluidic devices. COC has exhibited a unique combination of properties including an excellent UV transparency, a strong resistance to a wide range of chemicals and solvents and negligible moisture absorption. Another attribute of COC has been the ability to tailor its thermal and mechanical properties by variation in the ratio of cyclic monomer (typically norbornene) to olefin (ethylene) [1]. In copolymers with $\leq 40\%$ norbornene, the chemical structure of COC has been identified by nuclear magnetic resonance as comprising alternate sequences of norbornene and ethylene molecular units within the backbone of the main polymer chain [2]. Higher norbornene contents have acted to stiffen the main chain with the substitution of ethylene units by the bulky ring structure. As a consequence, an increase in norbornene content in COC has correlated with a linear rise in glass transition temperature, T_g [3], an increase in microhardness [4] and tensile strength [4] and a decrease in ductility [5]. The linear dependence of T_g on composition was shown by Forsyth et al. [6] as sensitive to the type of microstructure in the copolymer at high norbornene content.

COC has recently been used in the replication of microfluidic devices by the processes of hot embossing [7, 8] and injection moulding [9, 10]. In these studies, a number of different compositions of copolymer have been applied in the fabrication of channel structures. However, little systematic data exist on the effect of comonomer content in the replication of micropatterns in COC. This paper has examined both the dynamic mechanical behaviour and the hot embossing properties of a series of standard grades of COC. The norbornene/ethylene compositions of the copolymers were selected as providing a wide range of T_g. All grades have been synthesised using a common metallocene catalyst. Measurements of thermal deformation properties of the copolymers have been combined with the analysis of hot embossing characteristics. The temperature range in the vicinity of the glass transition has been selected in these experiments as widely used in the replication of microstructures during hot embossing [11]. The results of experiments on the optimisation of

P. W. Leech (✉) · X. Zhang
CSIRO Materials Science and Engineering,
Clayton 3168, VIC, Australia
e-mail: Patrick.Leech@csiro.au

Y. Zhu
CSIRO Materials Science and Engineering,
Highett 3193, VIC, Australia

embossing parameters have been applied in the fabrication of microfluidic channels.

Experimental details

The six commercial grades of Topas COC used in these experiments have been listed in Table 1. The copolymers contained a range of norbornene contents (61–82 wt%) as supplied by Polyplastics, Singapore. The level of incorporation of norbornene in COC has been previously reported by Forsyth et al. as directly dependent on the ratio of norbornene/ethylene in the copolymer [6]. The six grades have been designated as C-61 to C-82 in order to correspond to the wt% norbornene. Dynamic mechanical thermal analysis (DMTA) was performed on samples using a PerkinElmer PYRIS^{TM} system in dual cantilever bending mode. During DMTA, a plate specimen with dimensions of $10 \times 100 \times 1$ mm^3 was heated at a rate of 2.0 °C min^{-1} while applying a sinusoidally varying strain. The elastic storage modulus, E', loss modulus, E'', and loss factor, tan δ, were simultaneously determined at frequencies of 0.1, 0.5, 1.0, 5 and 20 Hz. In addition, a series of experiments on the hot embossing of the copolymers were performed using a hydraulic press with platens of brass and a nickel shim as a die. The pattern of the channels was fabricated in dry film resist (Shipley 5038) in a collimated UV system at 16.5 W/cm^2 ($\lambda = 350$–450 nm). The master pattern in resist was replicated as a Ni shim (hardness of ~ 265 HV) using an initial sputter deposition of 100 nm followed by electroplating in a nickel suphamate bath to a thickness of 150 nm. Hot embossing of the channel pattern was performed at a temperature of 80–180 °C and a force of 25 kN.

Results and discussion

Dynamic mechanical thermal analysis

Figure 1(a–c) shows plots of E', E'' and tan δ versus temperature in the range 20–200 °C. Each curve in Fig. 1(a) has exhibited a rapid decrease in E' above a critical temperature. A single α relaxation of this type has previously been attributed to the glass transition in COC [4, 6]. T_g was
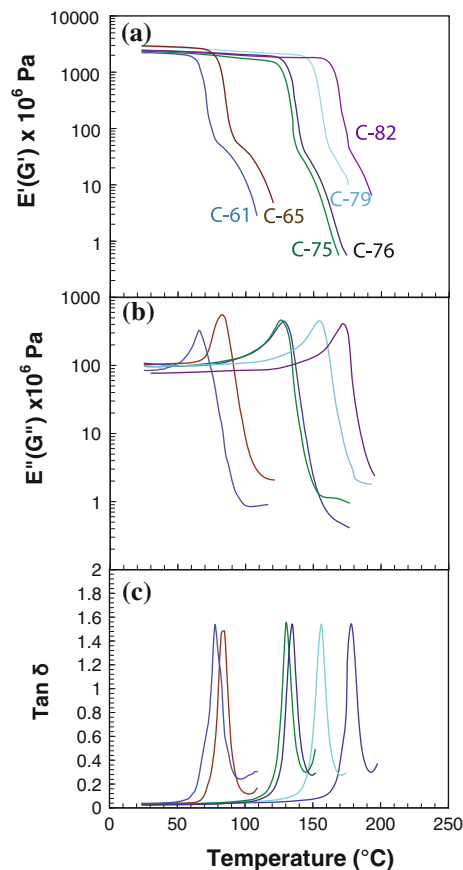

Fig. 1 **a** E', **b** tan δ and **c** E'' versus temperature obtained from DMTA. The tests on the six grades of COC were performed at 1 Hz

also evident as maxima in E'' and tan δ in Fig. 1(b) and (c), respectively. The temperature corresponding to the maximum in tan δ in Fig. 1(c) increased directly with % norbornene, although the intensity of the maximum remained constant at tan $\delta \sim 1.4$ in all grades. To determine the activation energy for the relaxation process, the frequency dependence (0.1–20 Hz) of the peak in tan δ was measured in the grades of COC. The semi-logarithmic plot of frequency versus inverse of temperature has given the apparent activation energy for these copolymers of $\Delta H = 650$ kJ mol^{-1}. This figure was consistent with the earlier value of $\Delta H = >400$ kJ mol^{-1} for the α transition in COC which was reported by Forsyth et al. [3, 4]. Figure 2 shows the temperature of the α relaxation plotted as a function of % norbornene. In this plot, the primary α relaxation was measured by the peak temperature in each

Table 1 Designation of samples in relation to grades of Topas COC

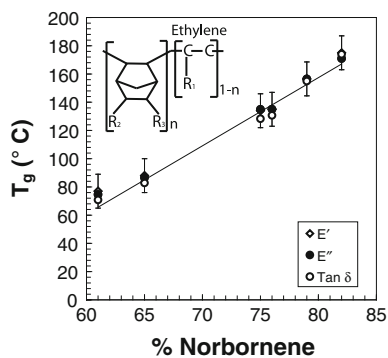| Sample	C-61	C-65	C-75	C-76	C-79	C-82
Norbornene wt%	61	65	75	76	79	82
COC Grade	9506F−04	8007S−04	5013L−10	6013 × 12	6015S−04	6017S−04

Fig. 2 Glass transition temperature as a function of % norbornene obtained from DMTA at a frequency of 1 Hz. The inset shows a unit of the chemical structure of the copolymers

of the plots of tan δ and E'' and by the end-point in plots of E'. A linear dependence of T_g on % norbornene has been previously reported by Shin et al. [2], Forsyth et al. [3], and Huang et al. [12] each using a series of COC which was synthesized with a single catalyst. Also shown in Fig. 2 is an inset showing the molecular structure of COC. The cyclic structure has been identified as containing repeat units of both the olefin monomer (with fraction of n) and ethylene $(1 - n$ fraction). The side branches were designated as R_1, R_2 and R_3 and comprised of $–C_nH_{2n+1}$ [13].

Oh and Inoue have concluded that the main chain in COC became less flexible with increasing norbornene content due to steric hindrance between the bulky structural units of cyclic olefin [13]. Hence, the trend of increase in T_g with norbornene content (Fig. 2) has been attributed to the increased resistance to relative sliding movement between the main chains with a greater density of cyclic monomer units [6]. At room temperature, the value of the elastic storage modulus, E', was measured in the range 2.3–3.0 × 10^9 Pa within the six grades of COC. As a general trend, the E' modulus increased with norbornene content at room temperature. Figure 1(a) also shows the sharp decrease in E' at T_g for each of the respective grades. At 40 °C above the transition, E' had decreased to 0.2–1.6 × 10^6 Pa, a drop in elastic modulus of more than three orders of magnitude from room temperature. The plot of E' versus temperature for each copolymer in Fig. 1(a) has also shown a slight change in slope at the upper limit of the transition. This variation in slope was a very weak indication of a plateau region in E' which has been indicative of rubbery flow in amorphous polymers [11, 14]. Rubbery flow above T_g has been identified as the elastic stretching of chain segments which were fixed within a network of entanglements [11]. However, the continuous and rapid decrease in E' which was evident at temperatures above T_g and the change in slope in Fig. 1(a) has indicated
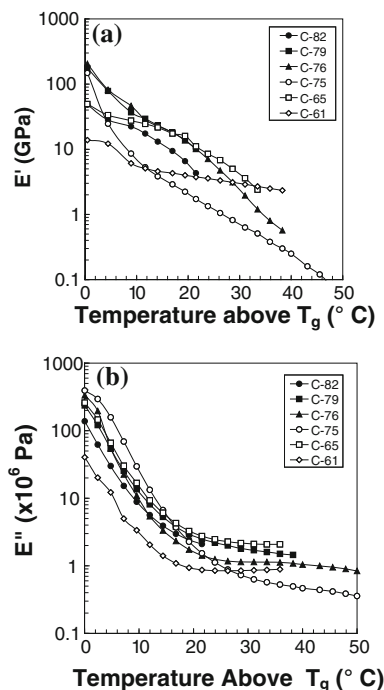

Fig. 3 a E' and b E'' plotted versus °C above the transition for each grade of COC. The measurements were performed at 1 Hz

that all of the grades of COC had transformed almost directly from the glass transition region to a regime of viscous liquid flow. This regime (viscous liquid flow) has been previously characterised by an irreversible deformation of the polymer together with a storage modulus of $E' \sim 10^5$–10^6 Pa, the value of E' depending on polymer species and concentration [11, 14].

Figure 3(a) and (b) shows the variation in the storage modulus, E', and loss modulus, E'', in the range of temperature immediately above T_g, respectively. The transition temperature used in plotting of Fig. 3(a) and (b) was the peak in tan δ for each copolymer. The scale of temperature used in Fig. 3(a) was standardised with respect to T_g for each grade of COC. Figure 3(a) shows that the elastic modulus, E', decreased exponentially above T_g for each of the grades of COC. A slight change in slope was evident in each plot at 10–20 °C above T_g. The exception to this trend was C-61 grade which exhibited a lower slope in E' versus temperature than other grades. At any given temperature above T_g, the range in E' between the grades of COC was within a band in which the upper and lower limits varied by approximately an order of magnitude. Over the range of temperatures in Fig. 3(a), the modulus E' was not directly related to % norbornene. In the viscous liquid flow state, the elastic constant was evidently independent of the composition of the cyclic units present in of the polymer backbone.

Figure 3(b) shows the loss modulus, E'', plotted versus temperature above T_g. The magnitude of E'' decreased sharply with increase in temperature before saturating at ~ 20 °C above T_g. The same trend was evident for all grades of COC as a function of temperature, with no direct correlation between E'' and % norbornene at temperatures within the saturation region. Evidently, the resistance to sliding of entire chain segments at temperatures above the transition was uninfluenced by the ratio of norbornene/ethylene in the structure. The constant value of E'' with increasing temperature at ≥ 20 °C above T_g indicates that the viscous deformation proceeding through the sliding of chain segments was essentially independent of temperature in this range.

The temperature range of 20–40 °C above the transition has been widely used in the hot embossing of polymers [11]. The results of DMTA in Figs. 1–3 have shown an optimal range of temperature of ≥ 20 °C above the transition for embossing of all the grades of COC. In this range, a negligibly small value of elastic modulus, E' was combined with a low and temperature invariant value of loss modulus, E''. This combination of parameters has enabled the hot embossing of COC essentially without residual elastic deformation and with a low energy loss due to viscous liquid flow.

Hot embossing experiments

Figures 4 and 5 show SEM images and profilometric traces of 200 μm wide channels after embossing in the C-61 and C-82 grades, respectively. The channels were embossed at the lower, mid-point and upper temperature in the transition range. At the lower temperature limit of the transition (30 °C) for C-61 grade, Fig. 4(a) shows a broad region of edge roughness along the channel together with some evidence of delamination. The edge region was visible only on the upper side of Fig. 4(a) because of a slight y-axis tilt applied to the sample.

The corresponding profile has shown a convex distortion at the base of the channel due to uneven recovery by elastic deformation following the viscoelastic flow. At the mid-temperature in the transition range (60 °C), Fig. 4(b) shows a reduction in the width of the edge roughness region combined with an increase in the embossed depth. Delamination at the edge of the channel and distortion at the base were also evident at this temperature. At the upper limit of the transition temperature at 90 °C, Fig. 4(c) shows a smooth sidewall with a narrow region of deformed edge. The depth of embossing was significantly greater at this temperature than below the transition, with formation of an essentially flat base in the channel. A slight ridge was present (see profile in Fig. 4c) due to displacement of polymer on either side of the channel. A similar pattern of deformation as a function of temperature through the transition range was also evident in the other grades of COC. However, in COC grades with higher norbornene content (C-79 and C-82), the formation of multiple cracks was evident along the length of the channel after embossing at temperatures below the transition. Cracks of this type, as visible in Fig. 5(a), were absent during embossing at higher temperatures above T_g (Fig. 5c). The formation of fibrillated crazes has been previously identified during the
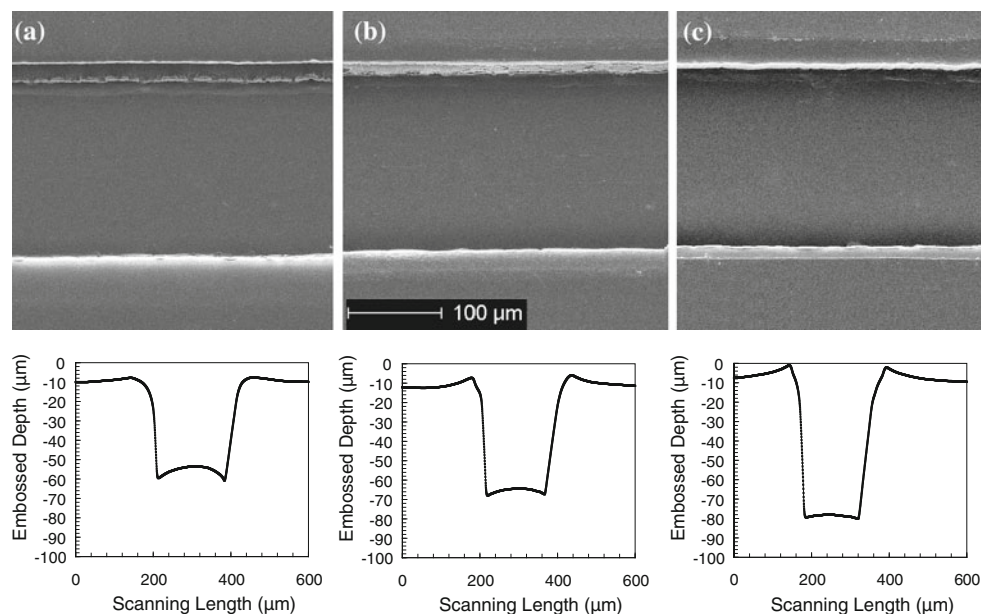

Fig. 4 Scanning electron micrographs and profilometry traces of channels embossed in C-61 grade at **a** 30 °C, **b** 60 °C, and **c** 90 °C at 25 kN force and 120 s duration

Fig. 5 Scanning electron micrographs and profilometry traces of channels embossed in C-82 grade at **a** 110 °C, **b** 140 °C, and **c** 170 °C at 25 kN force and 120 s duration
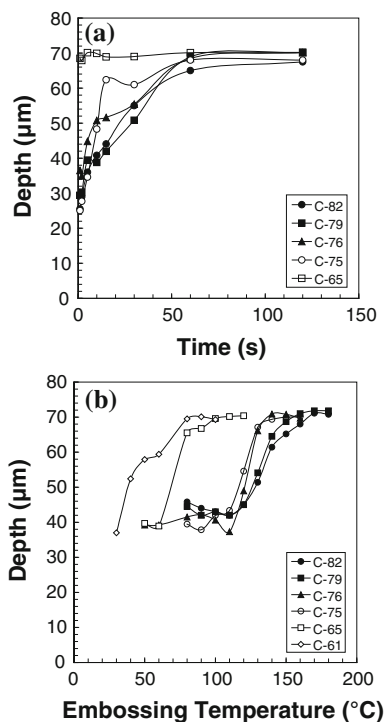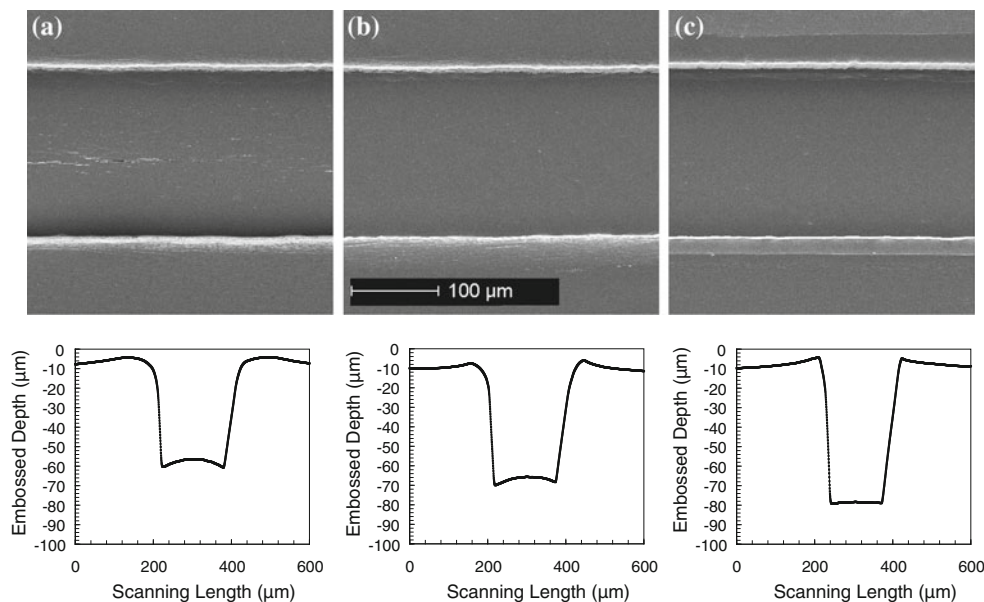

Fig. 6 **a** Embossing depth versus time at 170 °C and 25 kN force and **b** embossing depth versus temperature at 25 kN force and 120 s

deformation of COC with higher levels of % norbornene (68–78 wt%) [4]. An increase in norbornene content has been correlated with reduction in ductility of COC [4].

Figure 6(a) and (b) shows plots of the depth of embossing in 200-μm wide channels as a function of duration of loading and process temperature, respectively. In Fig. 6(a), the curve for each grade has shown a steep rise in depth with increase in embossing time until reaching an

approximately constant value at ∼60 s. The maximum depth of 70 μm was equivalent to the height of the ridge in the nickel shim. Figure 6(a) shows that, at embossing times of ≤60 s, a wide variation in depth was evident between the grades of COC. In general, the embossed depth increased with a reduction in % norbornene. Based on Fig. 6(a), an embossing time of 120 s was used as a standard procedure for the experiments.

Figure 6(b) shows that for each of the COC grades, the embossed depth has increased sharply over a critical range of temperature. At temperatures below the critical transition range, the depth of embossing was approximately constant at 40–50 μm. At temperatures above the critical range, the embossed depth increased to a plateau level of ∼70 μm, which was equivalent to the ridge height in the shim. Figure 6(b) shows that the transition temperature increased with norbornene content of the copolymers. This dependence of transition temperature on % norbornene was equivalent in both hot embossing and DMTA experiments. The lower limit of T_g was detected in hot embossing experiments at a slightly lower temperature than in DMTA. In comparison, the upper limit of the transition was similar for both embossing experiments and DMTA. The observed trend in transition temperature with % norbornene in Fig. 6(b) has been attributed to an increased level of interchain steric hindrance with increasing fraction, n, of the olefin structural units. The bulky and stiff side-groups in the olefin units act to resist the sliding motion of entire chains which determines the onset of viscous liquid flow [11].

All embossing experiments which were performed in the vicinity of the transition range of temperature resulted in the presence of a permanent deformation. However,

a temperature above the glass transition was required for the full definition of the channel without a distortion of the COC due to a residual elastic deformation. In the range of temperature of 20 °C above T_g, both the elastic modulus, E', and the loss modulus, E'', had decreased to 1–10 × 10^6 Pa and E'' was approximately constant with temperature. In this region of viscous liquid flow above T_g, the deformation during hot embossing was less sensitive to variation in temperature than within the transition range.

Conclusions

The dynamic mechanical behaviour of a series of norbornene/ethylene copolymers in the vicinity of the glass transition temperature has shown a linear dependence of T_g on % norbornene in COC. At temperatures above the transition in each grade, the magnitude of the elastic storage modulus, E', has decreased exponentially with temperature. At 40 °C above the transition, E' had decreased to a value in the range of 0.2–1.6 × 10^6 Pa, more than three orders of magnitude below E' at room temperature. The loss modulus, E'', has also decreased sharply with temperature before saturating at an approximately constant level at temperatures of ≥ 20 °C above T_g. In this range of temperature, the deformation of COC was characterised by a very low elastic modulus and a low and temperature independent value of loss modulus. The hot embossing of microchannels in all grades of COC in a regime of viscous liquid flow above T_g has produced smooth sidewalls, a flat base and full depth. A similar dependence of transition temperature on % norbornene was measured during both hot embossing and DMTA experiments.

References

1. McNally D (2003) In: Mark HF (ed) Encyclopedia of polymer science and technology, Vol. 2, 3rd edn. Wiley, Hoboken, NJ, 489 p
2. Shin JY, Park JY, Liu C, He J, Kim SC (2001) Pure Appl Chem 77(5):801
3. Forsyth JF, Scrivani T, Benavente R, Marestin C, Perena JM (2001) J Appl Polym Sci 82:2159
4. Scrivani T, Benaventure R, Perez E, Perena JM (2001) Macromol Chem Phys 202:2547
5. Seydewitz V, Krumova M, Michler GH, Park JY, Kim SC (2005) Polymer 46:5608
6. Forsyth JF, Perena JM, Benavente R, Perez E, Tritto I, Boggioni L, Brintzinger H-H (2001) Macromol Chem Phys 202:614
7. Cameron NS, Roberge H, Veres T, Jakeway SC, Crabtree HJ (2006) Lab Chip 6:936
8. Steigert J, Haeberle S, Brenner T, Müller C, Steinert CP, Koltay P, Gottschlich N, Reinecke H, Rühe J, Zengerle R, Ducré J (2007) J Microm Microeng 17:333
9. Hong C-C, Choi J-W, Ahn CH (2004) Lab Chip 4:109
10. Mair DA, Geiger E, Pisano AP, Fréchet JMJ, Svec F (2006) Lab Chip 6:1346
11. Guo LJ (2004) J Phys D Appl Phys 37:R123
12. Huang W-J, F-C Chang J, Chu PP-C (2000) J Polym Res 7(1):5
13. Oh GK, Inoue T (2005) Rheol Acta 45:116
14. Bicerano J (2002) Prediction of polymer properties, 3rd edn. Marcel Decker, NY, USA, p 169